ORIGINAL RESEARCH

Characterization of Carotid Atherosclerosis and Detection of Soft Plaque with Use of Black-Blood MR Imaging

K. Yoshida
O. Narumi
M. Chin
K. Inoue
T. Tabuchi
K. Oda
M. Nagayama
N. Egawa
M. Hojo
Y. Goto
Y. Watanabe
S. Yamagata

BACKGROUND AND PURPOSE: In the treatment of carotid atherosclerosis, the rate of stenosis and characteristics of plaque should be assessed to diagnose vulnerable plaques that increase the risk for cerebral infarction. We performed carotid black-blood (BB) MR imaging to diagnose plaque components and assess plaque hardness based on MR signals.

MATERIALS AND METHODS: Three images of BB-MR imaging per plaque were obtained from 70 consecutive patients who underwent carotid endarterectomy (CEA) to generate T1- and T2-weighted images. To evaluate the relative signal intensity (rSI) of plaque components and the relationship between histologic findings and symptoms, we prepared sections at 2-mm intervals from 34 intact plaques. We then calculated the relative overall signal intensity (roSI) of 70 plaques to assess the relationship between MR signal intensity and plaque hardness and symptoms.

RESULTS: The characteristics of rSI values on T1- and T2-weighted images of fibrous cap (FC), fibrosis, calcification, myxomatous tissue, lipid core (LC) with intraplaque hemorrhage (IPH), and LC without IPH differed. Symptomatic plaques were associated with FC disruption ($P < .001$) and LC with IPH ($P < .05$). The roSI on T1-weighted images was significantly higher for soft than nonsoft plaques. When the roSI cutoff value was set at 1.25 (mean of the roSI), soft plaques were diagnosed with 79.4% sensitivity and 84.4% specificity. The roSI was also significantly higher for symptomatic than for asymptomatic plaques. Soft and nonsoft plaques as well as symptomatic and asymptomatic plaques did not significantly differ on T2-weighted images.

CONCLUSION: BB-MR imaging can diagnose plaque components and predict plaque hardness. This procedure provides useful information for planning therapeutic strategies of carotid atherosclerosis.

Carotid atherosclerosis accounts for a large proportion of the causes of cerebral infarction, and accurate diagnostic imaging of carotid stenosis is useful for clarification of the pathogenesis of cerebral infarction and planning of therapy. In the diagnostic imaging of carotid arterial lesions, luminography such as conventional angiography is generally performed to determine the rate of stenosis, and in randomized studies documenting the value of carotid endarterectomy (CEA) in the treatment of carotid atherosclerosis, therapeutic guidelines have been based on stenosis rate.[1-3] Recent studies have also shown the critical importance of diagnosing vulnerable plaques, which are associated with a higher risk for cerebral infarction, by imaging the carotid artery wall itself and determining plaque characteristics.[4,5] Therefore, less invasive and more accurate diagnostic modalities such as carotid ultrasonography (US) for plaque evaluation have considerable importance in the management of patients with carotid atherosclerosis. Carotid US has been widely applied to characterize atherosclerotic plaque, and the content of soft plaque (lipid and hemorrhage) is presently associated with echolucency.[6,7] Furthermore, accumulating evidence indicates that echolucent plaques represent biologically more active disease and are associated with the risk for future stroke.[8,9] In addition, although carotid artery stent placement (CAS) is becoming an increasingly popular alternative to CEA in the treatment of carotid stenosis, several reports have shown that soft plaques are associated with a high incidence of ischemic complication during CAS.[10-12] Therefore, accurate diagnosis of carotid soft plaque seems to be of paramount clinical importance. However, carotid US has some limitations because it is difficult to obtain full images on patients who have a short neck, high carotid bifurcation, or highly calcified plaques.[13]

The chemical composition and physical properties of tissues can be determined by MR imaging, which indicates that this diagnostic technique should be useful in plaque characterization. Along with recent advances in imaging devices and techniques, many studies have documented the usefulness of high-resolution MR imaging in the diagnosis of plaque.[14-21] In addition to sorting plaque composition on the basis of MR signal intensity, if soft plaque can be differentiated from nonsoft plaque by overall plaque MR signal intensity, MR imaging will be a simple, objective, and useful method to diagnose carotid atherosclerosis. To our knowledge, however, few studies have closely assessed the MR imaging signals of plaque components by comparing CEA specimens with carotid MR imaging in vivo,[22] and the findings on MR imaging of carotid soft plaque have not been described.

Our study investigates the benefit of carotid black-blood (BB) MR imaging by evaluating the MR signal intensity of the components of carotid plaque and by detecting soft plaque on the basis of overall plaque MR signal intensity.

Methods

Study Population

We examined 70 consecutive patients (61 men, 9 women; median age, 69 years; age range, 53–80 years; symptomatic, 48) who underwent

Received April 27, 2007; accepted after revision December 31.

From the Departments of Neurosurgery (K.Y., O.N., M.C., M.H., Y.G., S.Y.), Cardiology (K.I.), Radiology (T.T., K.O., M.N., Y.W.), and Neurology (N.E.), Kurashiki Central Hospital, Okayama, Japan.

Please address correspondence to Kazumichi Yoshida, Department of Neurosurgery, Kurashiki Central Hospital, 1-1-1 Miwa Kurashiki-shi, Okayama 710, Japan; e-mail: ky7694@kchnet.or.jp

DOI 10.3174/ajnr.A1015

CEA for the treatment of atherosclerotic carotid artery stenosis at our hospital. Symptomatic patients were defined as those who have experienced amaurosis fugax, a transient ischemic attack, or a stroke in the territory of the ipsilateral carotid artery within 6 months. The severity of carotid artery stenosis was evaluated by digital subtraction angiography with the North American Symptomatic Trial Collaborators criteria,[3] and the rate of stenosis was 76.7 ± 1.8% (average ± SD). The inclusion criteria for CEA comprised more than 70% symptomatic and asymptomatic carotid stenoses or more than 50% symptomatic stenoses with recurrent infarcts on the ipsilateral hemisphere refractory to maximal medical treatment. With respect to risk factors for cerebral infarction, the prevalence of hypertension, diabetes, hypercholesterolemia, and coronary heart disease was 72%, 31%, 39%, and 32%, respectively.

The local institutional review board approved this study, and all patients provided written informed consent to participate in all procedures associated with the study.

MR Imaging

We performed carotid MR imaging using a 1.5T MR imaging machine (Gyroscan Intera; Philips Medical Systems, Best, the Netherlands) equipped with an 8-cm diameter surface coil. Data were collected from electrocardiogram-gated BB images during the end-diastolic phase when vascular pulsation was minimal. All patients underwent BB-MR imaging within 2 weeks before surgery. A long-axis image of the carotid artery, including a stenotic lesion, was obtained from the BB 3D gradient-echo sequence, and three T1- and T2-weighted short-axis turbo spin-echo (TSE) images of the artery, including the area with the highest stenotic rate for plaque characterization, were obtained on the basis of the long-axis image. The chemical shift selective fat suppression technique of spectral presaturation with inversion recovery (IR) was applied to all BB sequences to suppress excessive MR hyperintensity due to subcutaneous fat tissue. The parameters for the imaging sequences were as follows: long-axis T1-weighted images (3D IR turbo field echo): TR, 10; TE, 2.7; TI, 500; flip angle (FA), 35; 320 × 512 matrix; 1.6-mm section thickness; 150-mm FOV; short-axis T1-weighted images (2D double IR-TSE): TR, 700–1000; TE, 12; FA, 110; 256 × 256 matrix; 3 mm-section thickness; 150-mm FOV; TR, 1 cardiac cycle (1 R-R interval); short-axis T2-weighted images (2D double IR-TSE): TR, 1500–2000; TE, 80; FA, 90; 256 × 256 matrix; 3-mm section thickness; 150-mm FOV; TR, 2 cardiac cycles (2 R-R interval).

For short-axis images, the inversion time was the null-point of blood calculated with the following formula:

$$\text{null-point of blood} = \text{T1 blood}^{*} (\ln 2\text{-}\ln \{1 + \exp(-\text{TR}/\text{T1 blood})\})$$

$$\text{T1 blood} = \text{T1 value of blood (1200 ms)}.$$

The quality of the MR images of the carotid artery was assessed by an observer (N.E.), who did not participate in additional analysis of the MR imaging and histologic findings. We excluded MR images of the carotid arterial wall and lumen that were poorly outlined because of motion artifacts and flow artifacts from the study.

Plaque Excision and Histologic Processing

Specimens were excised by CEA without placement of an incision whenever possible for precise comparison of the MR image with the histologic section, and the MR signal intensity of the plaque components was analyzed only with intact plaques. When plaques could not be excised without damage, an additional incision was positioned for internal observation, histologic processing, and analysis of plaque hardness.

Specimens were fixed in formaldehyde, demineralized, and then embedded in paraffin. Plaques from each specimen were sectioned at 2-mm intervals, and then serial 5-μm-thick sections from each carotid slab were mounted for comparison with the MR images. Furthermore, sections that matched the MR imaging findings were visualized by staining with hematoxylin-eosin, Masson trichrome, and van Gieson elastic.

Matches Between MR Imaging and Histologic Findings

To measure the MR signal intensity of the plaque components, the MR imaging and histologic findings were precisely compared in 34 specimens that were excised by CEA without placement of an incision in the inner structures of the plaques. We selected sections of plaques corresponding to short-axis MR images based on factors such as distance from the bifurcation of the common carotid artery and the size and shape of the lumen and plaque.

Major components in the selected sections of histologically stained tissues were classified according to Virmani et al[23] by a colleague (K.I.), who was not informed of the MR imaging findings, as fibrous cap (FC), fibrosis mainly consisting of collagen fibers, calcification, myxomatous tissue rich in smooth muscle cells and extracellular matrix such as proteoglycans, lipid core (LC) with relatively fresh and broad intraplaque hemorrhage (IPH), and LC without IPH.

Relatively fresh IPH was defined as plaque components containing hemorrhagic debris and intact or degenerating red blood cells, but without a histologic tissue reaction.

Regions of interest (ROIs) identified as representing FC, fibrosis, calcification, myxomatous tissue, and LC with and without IPH were selected on each histologic section. For each plaque component, a manual operator-defined ROI was drawn on a workstation referring to the histologic features, and the signal intensity at the corresponding location on the matched MR image was measured. Relative signal intensity was then measured for the above 6 plaque components relative to the sternocleidomastoid muscle on T1-weighted images and the submandibular gland on T2-weighted images. Relative signal intensity was calculated with the following formula:

$$\text{rSI} = \text{SI component}/\text{SI ref},$$

(where rSI indicates relative signal intensity; SI, signal intensity; ref, reference tissue).

Relationship Between Histologic Findings and Symptoms

Relationships between histologic findings and carotid cerebrovascular events were investigated in sections taken at 2-mm intervals from 34 intact specimens as we have described previously ("Matches Between MR Imaging and Histologic Findings"). We compared FC disruption, fibrosis, calcification, myxomatous tissue, and LC with and without IPH between symptomatic and asymptomatic patients.

Correlation Between MR Signal Intensity and Plaque Hardness

We investigated whether plaque hardness could be estimated on the basis of MR signal intensity in 70 CEA specimens. We measured relative overall plaque MR signal intensity with manual operator-defined ROIs drawn over the whole plaque except for the lumen on short-axis MR images of areas with the highest rate of stenosis. As we have described previously, the reference tissue was the sternocleido-

mastoid muscle on T1-weighted images and the submandibular gland on T2-weighted images.

Relative overall plaque MR signal intensity was calculated with the following formula:

$$\text{roSI} = \text{SI whole plaque} / \text{SI ref}$$

(where roSI indicates relative overall plaque signal intensity; SI, signal intensity; ref, reference tissue).

Plaque hardness was classified into 2 groups by a colleague, who was not informed of the MR findings, and on the basis of histologic results of sections of the most stenotic areas. Soft plaque was defined as a lesion containing fibrous tissue, myxomatous tissue, or calcification in less than 50% of the plaque area with the highest rate of stenosis. Nonsoft plaque was defined as plaque that contained fibrous tissue, myxomatous tissue, or calcification in 50% or more of the plaque area. Plaque hardness was compared with the roSI value.

Relationship Between MR Signal Intensity and Symptoms

We examined the relationship between MR signal intensity and the risk for cerebrovascular events in 70 patients, as we have described previously ("Correlation Between MR Signal Intensity and Plaque Hardness"). Differences in the roSI values on T1- and T2-weighted images between symptomatic and asymptomatic patients were assessed.

Data Analysis

We performed all statistical analyses using SPSS 12.0 for Windows (SPSS, Chicago, Ill). The relative MR signal intensity is expressed as mean ± SD. Statistical differences in the rSI of plaque components were analyzed by the Tukey multiple-comparison post hoc test for T1-weighted images and by Tamhane multiple-comparison test for T2-weighted images. We analyzed the statistical differences in the relationship between roSI and plaque hardness and symptoms using the Student *t* test. We applied the χ^2 test for independence to assess the influence of plaque components on symptoms and thus determine associations between histologic findings and symptoms. The level of significance was established at $P < .05$. We then calculated the sensitivity and specificity of the roSI in detecting soft plaque using histologic findings as the criterion standard.

Results

MR Signal Intensity of Plaque Components

Of the 34 intact plaques, 2 were excluded because of poor quality on MR imaging, and of the 96 MR images obtained from the remaining 32 patients, we analyzed 61 that were judged as matching histologic sections.

Based on the histologic findings of 61 sections that matched the MR images, we identified 154 major plaque components. We confirmed FC on 23 sections, fibrosis on 36, calcification on 11, myxomatous tissue on 7, LC with IPH on 50, and LC without IPH on 27.

On T1-weighted images, the rSI for FC was 0.702 ± 0.208; for fibrosis, 1.099 ± 0.312; for calcification, 0.717 ± 0.215; for myxomatous tissue, 1.201 ± 0.255; for LC with IPH, 1.569 ± 0.251; and for LC without IPH, 1.287 ± 0.225. On T1-weighted images, rSI significantly differed among most components, but not between FC and calcification, fibrosis and myxomatous tissues, fibrosis and LC without IPH, and myxomatous tissue and LC without IPH (Fig 1).

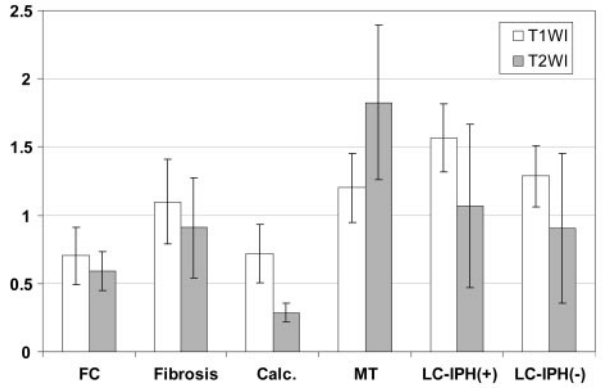

Fig 1. The rSI of plaque components on T1- and T2-weighted images. With use of specimens with matching MR images and excised plaque sections, the rSI of plaque components was calculated in relationship to the sternocleidomastoid muscle on T1-weighted images and the submandibular gland on T2-weighted images. On T1-weighted images, rSI significantly differed among most components, but not between FC and calcification, fibrosis and myxomatous tissues, fibrosis and LC without IPH, and myxomatous tissue and LC without IPH. On T2-weighted images, rSI significantly differed between FC and the other components except for LC without IPH, and between calcification and the other components. Bars indicate SD. FC indicates fibrous cap; Calc., calcification; MT, myxomatous tissue; LC-IPH(+), LC with intraplaque hemorrhage; and LC-IPH(-), LC without intraplaque hemorrhage.

Findings on MR imaging of plaque components

Histologic Features	T1-Weighted Images	T2-Weighted Images
FC	Hypointensity	Hypointensity
Fibrosis	Isointensity	Isointensity
Calcification	Hypointensity	Hypointensity
Myxomatous tissue	Isointensity	Hyperintensity
LC with IPH	Hyperintensity	Variable
LC without IPH	Isointensity	Variable

Note:—FC indicates fibrous cap; LC, lipid core; IPH, intraplaque hemorrhage.

On T2-weighted images, the rSI for FC was 0.590 ± 0.143; for fibrosis, 0.909 ± 0.369; for calcification, 0.287 ± 0.066; for myxomatous tissue, 1.826 ± 0.565; for LC with IPH, 1.070 ± 0.599; and for LC without IPH, 0.904 ± 0.546. On T2-weighted images, rSI significantly differed between FC and the other components except for LC without IPH, and between calcification and the other components (Fig 1).

The accompanying Table summarizes the findings on MR imaging of plaque components, and Figs 2, 3, and 4 show representative results.

Relationship Between Histologic Findings and Symptoms

Of the 34 specimens that were excised by CEA without placement of an incision in the inner plaque structures, 21 and 13 plaques were from symptomatic and asymptomatic patients, respectively. We confirmed FC disruption in 16 and 2 symptomatic and asymptomatic plaques, respectively. Fibrosis was the major component of 12 and 10 symptomatic and asymptomatic plaques, respectively; calcification in 11 and 6; myxomatous tissue in 7 and 3; LC with IPH in 20 and 8; and LC without IPH in 14 and 8, respectively. With respect to the association between carotid cerebrovascular events and the 6 plaque components, differences were significant only in FC disruption ($P < .001$) and in LC with IPH ($P < .05$) between symptomatic and asymptomatic patients.

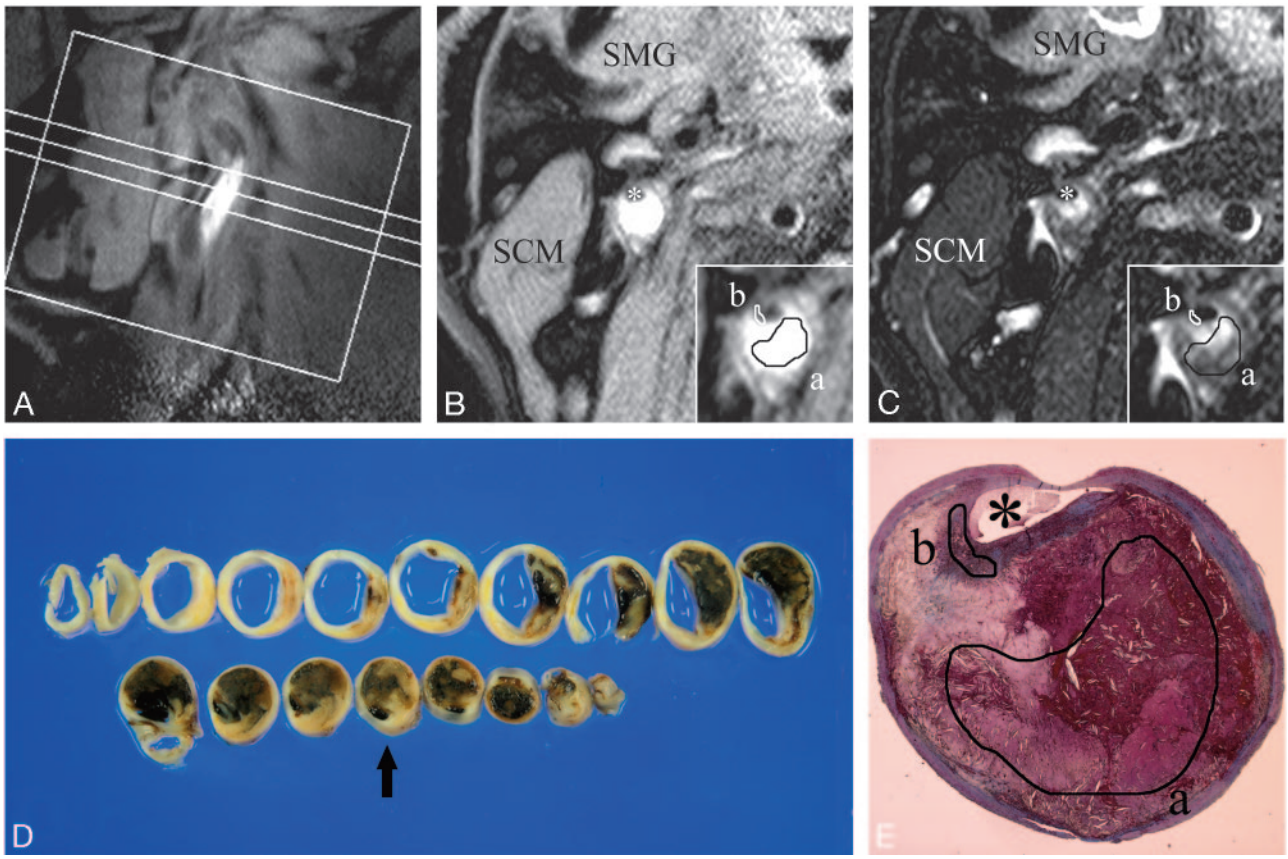

Fig 2. *A–E*, An example of MR images and histopathologic features of atherosclerotic plaque consisting of LC with intraplaque hemorrhage. First, a long-axis image of the carotid artery including a stenotic lesion was obtained (*A*), and based on this image, 3 T1-weighted and 3 T2-weighted short-axis images of the artery were obtained for plaque characterization. *B–C*, Axial T1- (*B*) and T2- (*C*) weighted images corresponding to the intermediate section in the long-axis image (*A*). *Inset*, a magnification of the atherosclerotic carotid plaque. A manual operator-defined ROI was drawn on a workstation to refer to the histologic features (*a*, LC-IPH(+); *b*, FC), and the rSI at the corresponding location on the matched MR image was measured. The rSI for LC-IPH(+) on T1- and T2-weighted images were 1.89 and 0.85, respectively. The rSI for FC on T1- and T2-weighted images were 0.71 and 0.53 in this case. SCM indicates sternocleidomastoid muscle; SMG, submandibular gland; asterisk, lumen. *D*, Gross sections of carotid endarterectomy specimen at approximately 2-mm intervals. A section corresponding to axial MR images (*B–C*) is marked with an arrow. *E*, Masson trichrome–stained cross section matched to axial MR images (*B–C*) showed an abundant LC-IPH(+) and FC (*a* and *b*, manual operator-defined ROIs for LC-IPH(+) (*a*) and FC (*b*).

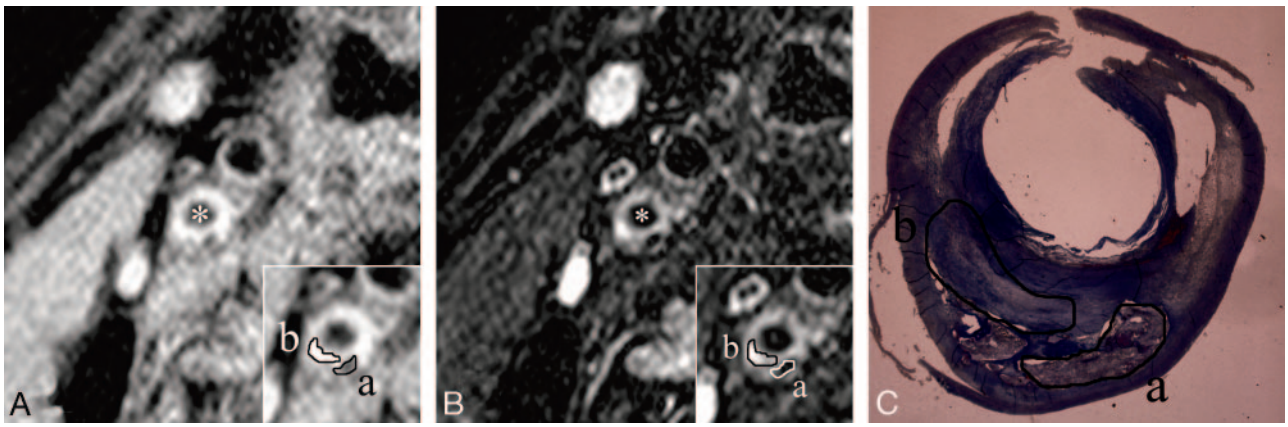

Fig 3. *A–C*, An example of MR images and histopathologic features of carotid plaque with mixed components. *A* and *B*, Short-axis T1- and T2-weighted images. *Inset*, a magnification of the atherosclerotic carotid plaque. With manual operator-defined ROIs for calcification (*a*) and fibrosis (*b*) as major components, the rSIs of calcification and fibrosis on T1-weighted images were 0.61 and 1.05, respectively. In the same way, the rSIs of calcification and fibrosis on T2-weighted image was 0.3 and 1.3, respectively. Asterisks indicate the lumen. *C*, Masson trichrome stained cross section matched to axial MR images (*A,B*) demonstrate so-called hard plaque composed of abundant collagen fibers (*b*) and calcification (*a*). Small intraplaque hemorrhage was also confirmed in this section.

Correlation Between MR Signal Intensity and Plaque Hardness

Of the 70 specimens, we excluded 4 because of poor MR image quality and thus analyzed 66 specimens comprising 32 soft and 34 nonsoft plaques on the basis of histologic findings. The roSI values of soft and nonsoft plaques on T1-weighted images were 1.47 ± 0.30 and 1.06 ± 0.25, respectively; the roSI of the soft plaques was significantly higher. These values did not sig-

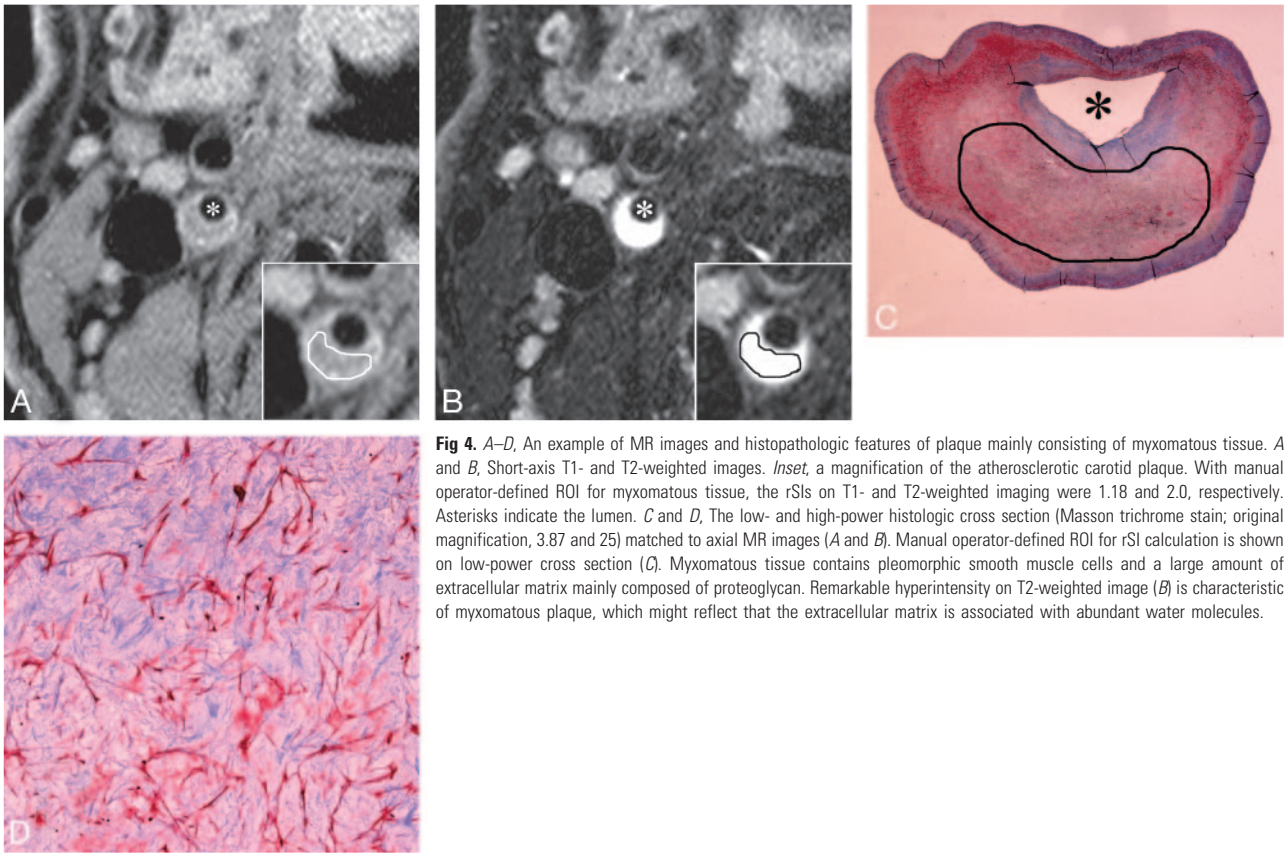

Fig 4. *A–D*, An example of MR images and histopathologic features of plaque mainly consisting of myxomatous tissue. *A* and *B*, Short-axis T1- and T2-weighted images. *Inset*, a magnification of the atherosclerotic carotid plaque. With manual operator-defined ROI for myxomatous tissue, the rSIs on T1- and T2-weighted imaging were 1.18 and 2.0, respectively. Asterisks indicate the lumen. *C* and *D*, The low- and high-power histologic cross section (Masson trichrome stain; original magnification, 3.87 and 25) matched to axial MR images (*A* and *B*). Manual operator-defined ROI for rSI calculation is shown on low-power cross section (*C*). Myxomatous tissue contains pleomorphic smooth muscle cells and a large amount of extracellular matrix mainly composed of proteoglycan. Remarkable hyperintensity on T2-weighted image (*B*) is characteristic of myxomatous plaque, which might reflect that the extracellular matrix is associated with abundant water molecules.

nificantly differ between the 2 groups on T2-weighted images (soft plaques, 0.90 ± 0.39; nonsoft plaques, 0.86 ± 0.32). When the roSI cutoff value on T1-weighted images was set at 1.25 (mean of roSI), the soft plaques were diagnosed with 79.4% sensitivity and 84.4% specificity.

Relationship Between MR Signal Intensity and Symptoms

We examined the relationship between symptoms and MR signals in 44 symptomatic and 22 asymptomatic patients. The roSI values from symptomatic and asymptomatic patients on T1-weighted images were 1.30 ± 0.35 and 1.15 ± 0.31, respectively, and those on T2-weighted images were 0.83 ± 0.30 and 0.98 ± 0.43, respectively. The roSI was significantly higher on T1-weighted images of symptomatic, rather than asymptomatic, patients, but the roSI on T2-weighted images did not significantly differ between the 2 groups.

Discussion

Plaque characteristics in addition to rate of stenosis play important roles in the diagnostic imaging of atherosclerotic lesions. In consideration of the onset risk for cerebral infarction in the carotid artery, not only the shape of the vascular lumen, but also the vascular wall, should be assessed.[5] Carotid US has been widely applied to characterize atherosclerotic plaque, though this procedure sometimes has limitations. Among the components of soft plaque, differentiation between IPH and the LC by carotid US is less robust, and plaque visualization itself can be incomplete when atherosclerosis is heavily calcified. The chemical composition and physical properties of tissue can be diagnosed by MR imaging with high-contrast resolution. Furthermore, image interpretation is highly objective compared with carotid US. Thus, MR imaging has been considered useful in plaque characterization, and many studies have examined findings on MR imaging associated with carotid plaques.[17-22,24,25]

Here, we confirmed the characteristic MR imaging findings of 6 plaque components and the ability of BB-MR imaging to accurately and noninvasively project histologic findings by combining the rSI values on T1- and T2-weighted images (Fig 1).

The status of FC has a major impact on the stability of plaques,[23,26,27] and its accurate assessment is of paramount clinical importance. The MR signals of FC were hypointense on both T1- and T2-weighted BB-MR imaging, which closely correlated with the histologic findings. However, taking into consideration that FC is attenuated collagen fiber adjacent to lumen, distinguishing between FC and lumen by BB-MR imaging might be difficult. Furthermore, when attenuated calcification, which appears as hypointensity on both T1- and T2-weighted images, is located close to FC, BB-MR imaging alone could not accurately characterize plaques. Therefore, the combination of BB-MR imaging and other sequences such as MR imaging with the 3D time-of-flight protocol reported by Hatsukami et al[28] seems necessary for precise FC evaluation.

The MR imaging findings of LC among different studies are inconsistent. This might be partly because the composition of tissues that are classified as LC obviously differs according to the stages of atherosclerotic changes. In particular, LC is often accompanied by IPH in advanced atherosclerotic lesions, which clearly affects MR imaging signals. Hematoma associated with intracerebral bleeding, which has a relatively even composition, differs from IPH in that IPH is uneven and

has a mixed LC content and blood components, and time after bleeding further complicates MR imaging findings of LC.[24] Many symptomatic lesions are accompanied by intraplaque hemorrhagic changes,[24,29-31] and we classified LC as that with and without IPH in our study. A remarkably high rSI on T1-weighted images was characteristic of LC with IPH.

Some myxomatous tissues can appear in plaques during tissue repair processes after FC rupture and also in restenotic tissue after endovascular therapy for stenotic lesions.[32,33] However, we found that plaque could sometimes be composed of myxomatous tissue (Fig 4), which was isointense on T1-weighted images and obviously hyperintense on T2-weighted images, reflecting water molecules captured by extracellular matrix components, mainly proteoglycan. From the viewpoint of the natural history of plaques mostly comprising myxomatous tissue, the stenotic rate can rapidly increase because many smooth muscle cells are highly polymorphic and proliferative.[33] Hence, even asymptomatic lesions require careful follow-up. In addition, even if CAS is performed on such patients, the predicted rate of restenosis will be high, and as a result, careful investigation is required in the event of obvious hyperintensity on T2-weighted images.

A thin or disrupted FC and IPH are important components of vulnerable atherosclerotic plaque.[34,35] Although the sample size was small, our study demonstrated that symptomatic plaques more frequently contained FC disruption and LC-IPH among 6 plaque components. Despite some limitations in the evaluation of FC status as noted above, BB-MR imaging seems to be useful in the detection of vulnerable plaques

A high roSI on T1-weighted images indicated soft plaques with a high degree of sensitivity and specificity. On the basis of the rSI of plaque components, high-average T1-weighted signal intensities indicated plaques comprising LC with a large quantity of relatively fresh IPH. Although the notion that soft plaque actually refers to LC is generally accepted, we postulate that the presence of broad IPH substantially indicates large LC because IPH is, in fact, uneven and coexists with LC on histologic sections. Although CAS has recently been developed as a potential alternative to CEA because it is less invasive, distal embolization from carotid plaque remains the most formidable complication of CAS. Several studies have demonstrated that soft plaques are associated with a high incidence of embolization during CAS.[10-12] Therefore, accurate and objective diagnosis of soft plaque with roSI of BB-MR imaging would be clinically useful for the planning of carotid revascularization. One possible problem with assessment of hardness by roSI is that soft plaques cannot be diagnosed when plaques are composed of large LC without IPH, because the rSI of LC without IPH is not necessarily high on T1-weighted images based on the rSI of plaque components.

The roSI on T1-weighted images was significantly higher in symptomatic than in asymptomatic plaques. This probably reflects the fact that vulnerable plaques are closely related to IPH.[34-36] Furthermore, the finding that the roSI on T1-weighted images was high in both soft and symptomatic plaques seems to be supported by several reports indicating a relationship between plaque hardness and vulnerability.[8,9] In contrast to T1-weighted images, the roSI of asymptomatic plaques on T2-weighted images tended to be high, though the difference did not reach significance. Thus, the rSI findings of plaque components indicate that asymptomatic plaques contain much myxomatous tissue, which emerges during healing after FC disruption and contributes to plaque stabilization.

Our study had several limitations. With respect to the parameters for BB imaging sequences, TR and TE in the T1-weighted sequences are relatively long for cardiac gating, and the proton concentration and T2 value of the tissue might influence T1 signal intensity. In a similar fashion, the relatively short TR and TE used in the T2-weighted sequence might influence T2 signal intensity. This is an unavoidable limitation for BB sequences, but it does not seem to constitute a serious disadvantage because the distribution of signal intensity on standard T1- and T2-weighted BB images still has practical value. One possible limitation of measuring T2-weighted MR signal intensity could be age-related variation in the signal intensity of the submandibular gland. Although the sternocleidomastoid muscle is generally the standard reference, the disadvantage is that the signal intensity of muscles on T2-weighted images is too low to obtain a reliable relative MR signal intensity. We used the submandibular gland as the internal reference because its signal intensity was constantly higher than that of the sternocleidomastoid muscle on T2-weighted images. With regard to the MR signal intensity of plaque components, we confirmed significant differences in rSI among many of them. However, the *P* value for differences might be overly optimistic because the numbers of MR sections obtained from each patient were unequal, and correlations among sections from the same patient were not taken into account.

We used a 1.5T MR instrument and a surface coil, which resulted in a spatial resolution of approximately 600 μm, but one of the diagnostic criteria for vulnerable carotid plaques is the presence of thin FCs that are less than 200 μm.[5] Hence, detecting thin FCs is presently difficult. Additional improvements in the spatial resolution of high-magnetic-field MR imaging might allow the future diagnosis of thin FCs. In scanning time, imaging that combines 2D SE and cardiac gating requires approximately 1 minute to obtain a single section. Therefore, to obtain several images of a single lesion is time consuming and difficult. Other investigations of plaques have shown that histologic findings can remarkably differ with only slight differences in location, and as in our study, plaque characterization might be insufficient if based on only 3 images per plaque. Also, evaluation of plaque hardness on the basis of roSI only for 1 MR section of the most stenotic area might not accurately reflect actual plaque hardness. Hence, an efficient plaque imaging technique on MR imaging should be established by a combination of 3D gradient-echo scanning with an even shorter scanning time.

Conclusions

Our study compared the BB-MR imaging findings with the histologic findings of CEA specimens. The results suggested that BB-MR imaging can diagnose plaque components and predict plaque hardness with a high degree of accuracy. This procedure provides very useful information not only for the planning of therapeutic strategies for carotid artery stenosis, but also for clarification of the pathogenesis and natural history of plaques.

Acknowledgments

We thank Ms. Kumi Nishida, Ms. Hiroko Suyama, and Ms. Yoshiko Matsumoto for preparing this manuscript and figures and Mr. Yoshiharu Yamamoto for statistical analysis.

References

1. **MRC European Carotid Surgery Trial: interim results for symptomatic patients with severe (70–99%) or with mild (0–29%) carotid stenosis. European Carotid Surgery Trialists' Collaborative Group.** *Lancet* 1991;337:1235–43
2. **Endarterectomy for asymptomatic carotid artery stenosis. Executive Committee for the Asymptomatic Carotid Atherosclerosis Study.** *JAMA* 1995;273:1421–28
3. **Beneficial effect of carotid endarterectomy in symptomatic patients with high-grade carotid stenosis. North American Symptomatic Carotid Endarterectomy Trial Collaborators.** *N Engl J Med* 1991;325:445–53
4. Naghavi M, Libby P, Falk E, et al. **From vulnerable plaque to vulnerable patient: a call for new definitions and risk assessment strategies: Part I.** *Circulation* 2003;108:1664–72
5. Wasserman BA, Wityk RJ, Trout HH 3rd, et al. **Low-grade carotid stenosis: looking beyond the lumen with MRI.** *Stroke* 2005;36:2504–13
6. El-Barghouty NM, Levine T, Ladva S, et al. **Histological verification of computerised carotid plaque characterisation.** *Eur J Vasc Endovasc Surg* 1996;11:414–16
7. Gronholdt ML, Nordestgaard BG, Wiebe BM, et al. **Echo-lucency of computerized ultrasound images of carotid atherosclerotic plaques are associated with increased levels of triglyceride-rich lipoproteins as well as increased plaque lipid content.** *Circulation* 1998;97:34–40
8. Gronholdt ML, Nordestgaard BG, Schroeder TV, et al. **Ultrasonic echolucent carotid plaques predict future strokes.** *Circulation* 2001;104:68–73
9. Lee RT, Loree HM, Cheng GC, et al. **Computational structural analysis based on intravascular ultrasound imaging before in vitro angioplasty: prediction of plaque fracture locations.** *J Am Coll Cardiol* 1993;21:777–82
10. Ohki T, Marin ML, Lyon RT, et al. **Ex vivo human carotid artery bifurcation stenting: correlation of lesion characteristics with embolic potential.** *J Vasc Surg* 1998;27:463–71
11. Henry M, Henry I, Klonaris C, et al. **Benefits of cerebral protection during carotid stenting with the PercuSurge GuardWire system: midterm results.** *J Endovasc Ther* 2002;9:1–13
12. Biasi GM, Froio A, Diethrich EB, et al. **Carotid plaque echolucency increases the risk of stroke in carotid stenting: the Imaging in Carotid Angioplasty and Risk of Stroke (ICAROS) study.** *Circulation* 2004;110:756–62
13. Chaudhuri TK, Fink S, Weinberg S, et al. **Pathophysiologic considerations in carotid artery imaging: current status and physiologic background.** *Am J Physiol Imaging* 1992;7:77–94
14. Görtler M, Goldmann A, Mohr W, et al. **Tissue characterisation of atherosclerotic carotid plaques by MRI.** *Neuroradiology* 1995;37:631–35
15. Yuan C, Mitsumori LM, Beach KW, et al. **Carotid atherosclerotic plaque: noninvasive MR characterization and identification of vulnerable lesions.** *Radiology* 2001;221:285–99
16. Quick HH, Debatin JF, Ladd ME. **MR imaging of the vessel wall.** *Eur Radiol* 2002;12:889–900
17. Yuan C, Kerwin WS. **MRI of atherosclerosis.** *J Magn Reson Imaging* 2004;19:710–19
18. Cai JM, Hatsukami TS, Ferguson MS, et al. **Classification of human carotid atherosclerotic lesions with in vivo multicontrast magnetic resonance imaging.** *Circulation* 2002;106:1368–73
19. Yuan C, Mitsumori LM, Ferguson MS, et al. **In vivo accuracy of multispectral magnetic resonance imaging for identifying lipid-rich necrotic cores and intraplaque hemorrhage in advanced human carotid plaques.** *Circulation* 2001;104:2051–56
20. Coombs BD, Rapp JH, Ursell PC, et al. **Structure of plaque at carotid bifurcation: high-resolution MRI with histological correlation.** *Stroke* 2001;32:2516–21
21. Honda M, Kitagawa N, Tsutsumi K, et al. **High-resolution magnetic resonance imaging for detection of carotid plaques.** *Neurosurgery* 2006;58:338–46
22. Cappendijk VC, Cleutjens KB, Kessels AG, et al. **Assessment of human atherosclerotic carotid plaque components with multisequence MR imaging: initial experience.** *Radiology* 2005;234:487–92
23. Virmani R, Kolodgie FD, Burke AP, et al. **Lessons from sudden coronary death: a comprehensive morphological classification scheme for atherosclerotic lesions.** *Arterioscler Thromb Vasc Biol* 2000;20:1262–75
24. Chu B, Kampschulte A, Ferguson MS, et al. **Hemorrhage in the atherosclerotic carotid plaque: a high-resolution MRI study.** *Stroke* 2004;35:1079–84
25. Kampschulte A, Ferguson MS, Kerwin WS, et al. **Differentiation of intraplaque versus juxtaluminal hemorrhage/thrombus in advanced human carotid atherosclerotic lesions by in vivo magnetic resonance imaging.** *Circulation* 2004;110:3239–44
26. Sitzer M, Müller W, Siebler M, et al. **Plaque ulceration and lumen thrombus are the main sources of cerebral microemboli in high-grade internal carotid artery stenosis.** *Stroke* 1995;26:1231–33
27. Carr S, Farb A, Pearce WH, et al. **Atherosclerotic plaque rupture in symptomatic carotid artery stenosis.** *J Vasc Surg* 1996;23:755–65
28. Hatsukami TS, Ross R, Polissar NL, et al. **Visualization of fibrous cap thickness and rupture in human atherosclerotic carotid plaque in vivo with high-resolution magnetic resonance imaging.** *Circulation* 2000;102:959–64
29. Moody AR, Murphy RE, Morgan PS, et al. **Characterization of complicated carotid plaque with magnetic resonance direct thrombus imaging in patients with cerebral ischemia.** *Circulation* 2003;107:3047–52
30. Murphy RE, Moody AR, Morgan PS, et al. **Prevalence of complicated carotid atheroma as detected by magnetic resonance direct thrombus imaging in patients with suspected carotid artery stenosis and previous acute cerebral ischemia.** *Circulation* 2003;107:3053–58
31. Lusby RJ, Ferrell LD, Ehrenfeld WK, et al. **Carotid plaque hemorrhage. Its role in production of cerebral ischemia.** *Arch Surg* 1982;117:1479–88
32. Volker W, Schmidt A, Oortmann W, et al. **Mapping of proteoglycans in atherosclerotic lesions.** *Eur Heart J* 1990;11:29–40
33. Matsuura R, Isaka N, Imanaka-Yoshida K, et al. **Deposition of PG-M/versican is a major cause of human coronary restenosis after percutaneous transluminal coronary angioplasty.** *J Pathol* 1996;180:311–16
34. Fryer JA, Myers PC, Appleberg M. **Carotid intraplaque hemorrhage: the significance of neovascularity.** *J Vasc Surg* 1987;6:341–49
35. Virmani R, Burke AP, Kolodgie FD, et al. **Vulnerable plaque: the pathology of unstable coronary lesions.** *J Interv Cardiol* 2002;15:439–46
36. Takaya N, Yuan C, Chu B, et al. **Association between carotid plaque characteristics and subsequent ischemic cerebrovascular events: a prospective assessment with MRI–initial results.** *Stroke* 2006;37:818–23